Optics Communications 356 (2015) 208–211

Contents lists available at ScienceDirect

Optics Communications

journal homepage: www.elsevier.com/locate/optcom

Light induced absorption and optical sensitizing of $Sn_2P_2S_6$:Sb

Yaroslav Skrypka [a], Alexandr Shumelyuk [a], Serguey Odoulov [a,*], Sergey Basun [b], Dean Evans [b]

[a] Institute of Physics, 46, Science ave., Kyiv 03650, Ukraine
[b] Air Force Research Laboratory, Materials and Manufacturing Directorate, Wright Patterson AFB, Dayton, OH 45433, USA

ARTICLE INFO

Article history:
Received 14 March 2015
Received in revised form
28 July 2015
Accepted 29 July 2015

Keywords:
Photorefractive nonlinearity
Optical sensitizing
Light induced absorption
Tin hypothiodiphosphate

ABSTRACT

Photorefractive sensitivity of antimony doped $Sn_2P_2S_6$ can be increased at ambient temperature by preexposure of the sample with an intense auxiliary light beam. It is shown that the largest enhancement of sensitivity occurs if the photon energy of preexposure light is close to the crystal bandgap, it decreases gradually with increasing wavelength. The preexposure gives rise also to a pronounced transient light induced absorption which vanishes approximately one order of magnitude faster than the decay of the sensitized state.

Published by Elsevier B.V.

1. Introduction

The fast response time, high gain factor, and broad spectral sensitivity, which is extended for some dopants up to telecommunication wavelength 1.5 μm, make Tin Hypothiodiphosphate ($Sn_2P_2S_6$, SPS) an attractive photorefractive material for numerous applications [1–4]. At the same time, the photorefractive response of SPS is still inhibited by the space charge field limitation, a consequence of the insufficient effective trap density [5]. In part, the problem of insufficient effective trap density was solved by technological efforts: crystals deliberately doped during the growth procedure showed improved characteristics [3,6,7]. There remains, however, still much room for further improvement, until the fundamental limit for the gain factor is reached, which is defined by the largest Pockels tensor component of SPS.

Other ways of reducing the space charge screening have been proposed too, which consist of (1) optimizing the interaction geometry (to profit from strong anisotropy of the low frequency dielectric permittivity) [8,9], and (2) influencing the effective trap density by preexposure of SPS samples to the auxiliary intense (incoherent or coherent) light beam [1,5]. The latter technique of SPS sensitizing appeared to be quite effective for antimony doped crystals [5], when the preexposure was achieved with the intense light of the same wavelength as the recording light (633 nm line of He–Ne laser which is traditionally used for photorefractive grating recording in SPS). It was established recently that the photogeneration of the secondary photorefractive centers is somehow related to recharging of the antimony defect center from an initially trivalent to a divalent state [10].

In this paper we intend to clarify, to what extent the sensitizing process depends on the wavelength of preillumination light and how the sensitizing process might be interrelated with the light induced absorption [11,12].

2. Experimental technique

Several $Sn_2P_2S_6$ samples grown in Uzhgorod National University (Ukraine) are tested in the experiment, SPS:Sb1% ($4.3 \times 3.7 \times 2.4$ mm^3, sample K21), SPS:Sb1% ($2 \times 3.5 \times 2$ mm^3, sample K24), SPS:Sb1% ($6.5 \times 8 \times 4$ mm^3, sample K33), SPS:Sb0.5%, Te0.5% ($3.34 \times 3.18 \times 1.26$ mm^3, sample K31), SPS:Te1% ($6.62 \times 7.32 \times 3.41$ mm^3, sample K32). The nominally undoped SPS ($10 \times 8 \times 6.5$ mm^3, sample K16) serves as a reference sample. All samples have been cut along the crystallographic axes with their *xy*-faces being optically finished.

Fig. 1 represents schematically the experimental set-up. The output beam from the He–Ne laser is impinged upon the SPS sample along its *z*-axis, nearly normally to the input face and the transmitted beam is directed to the detector D. This detector is placed far away from the sample to measure only the intensity of the small-diverging laser beam and avoid any scattered light. The polarizer P1 and lambda half phase retarder $\lambda/2$ allow for controlling the incident beam intensity while keeping its polarization always the same, parallel to the crystal *x*-axis. The preillumination

* Corresponding author.
E-mail address: odoulov@iop.kiev.ua (S. Odoulov).

http://dx.doi.org/10.1016/j.optcom.2015.07.077
0030-4018/Published by Elsevier B.V.

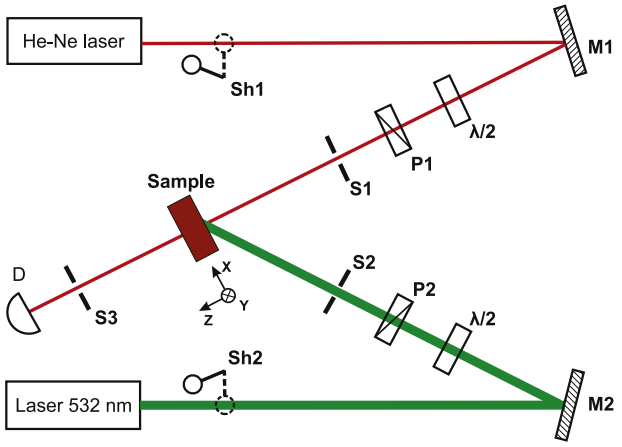

Fig. 1. Experimental set-up. The intensity of the test beam (He–Ne laser) transmitted through the sample is measured with the detector D, the signal from the detector is digitized and stored in a computer (not shown in this drawing). The auxiliary source (for example, frequency doubled cw Nd^{3+}:YAG laser, 532 nm) is used for preillumination. The mirrors M1,2 direct the laser beams to the SPS crystal, the polarizers P1,2 with phase retarders $\lambda/2$ control the laser beams intensities. The apertures S1,2,3 control the beam diameters and cut off the scattered light. The shutters Sh1,2 allow for manipulating the testing and preillumination beams.

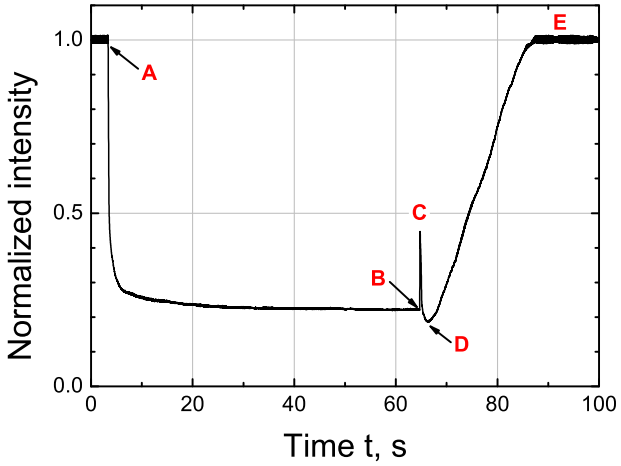

Fig. 2. Temporal variation of the red testing beam intensity in response to green light exposure for the sample K24. A and B mark the moments when green light is switched on and switched off, respectively. C, D, and E represent the moments where partial bleaching, strongest nonlinear scattering, and recovery practically to the initial transmission occur, respectively.

of the sample is accomplished with the light from an auxiliary source: the diode pumped frequency doubled Nd^{3+}:YAG laser with 532 nm output is shown in Fig. 1. This auxiliary source might be a He–Ne laser, a diode pumped solid state laser with 671 nm output, or a high-power LED with 585–595 nm output. The intensity of the preilluminating beam is controlled by polarizer P2 and one more lambda half phase retarder, the same way as it is done for the red testing beam. The angle between the testing beam and auxiliary source beam is 10–20° in order to ensure perfect overlap of two beams throughout the whole sample thickness.

The apertures S1 and S2 have a dual function: with their known diameters it is easy to evaluate the intensities of the two beams if the energies of the transmitted pulses are measured. On the other hand, by adjusting a small enough diameter of S1 one can be sure that the whole testing beam passes through preilluminated area of the sample. Two shutters, Sh1 and Sh2, are used to program the temporal sequences of testing and auxiliary illumination.

3. Experimental results

The main quantity measured in the experiment is a sample transmittance at the He–Ne laser wavelength, 633 nm. A standard procedure was to preilluminate the SPS sample for approximately a minute until a saturated state is reached, then after removing the auxiliary beam, measuring the intensity of transmitted testing beam.

Fig. 2 shows a representative example of temporal variation of the testing beam intensity with SPS:Sb 1% (K24) preexposure to the green light. The intensities of the testing beam and auxiliary beam are 55 mW/cm^2 and 2.8 W/cm^2, respectively. The intensity of the transmitted testing beam before the start of illumination with green light (moment A in Fig. 2) is taken as a reference, which is normalized to unity.

The onset of green illumination leads to a rapid decrease of the transmitted beam intensity which is due to the photoinduced absorption created by the green light. A complete saturation of transmission is reached after 60 s exposure, at which point the green light illumination is abruptly stopped (moment B in Fig. 2). A rapid partial bleaching of the sample starts after moment B. After a certain delay time, at moment C, the sample transparency drops once more reaching a minimum at moment D and then returns gradually with a much slower rate practically to the initial value at moment E. This second "darkening" of the sample is a consequence of the strong transient nonlinear scattering of the testing beam in SPS sample which is sensitized by the green illumination. The preillumination with the intense green light acts therefore in a similar way as formerly reported preillumination with the intense red light [5]: the photorefractive response becomes temporarily increased, the strong photorefractive scattering (beam fanning) develops which takes away a considerable part of the pump intensity. At moment D the transmitted pump beam becomes therefore depleted. For times longer than 100 s the sensitized state vanishes completely, crystal gain factor returns to its equilibrium value and sample transmission becomes the same as it was before preillumination. Depending on the intensity of green light preillumination the second minimum in temporal dependence of transparency, which is due to the transient beam fanning, can be less deep or more deep than the first one, which is due to nonlinear absorption. This scenario is typical for preillumination of antimony doped SPS with all other wavelengths too; particular cases differ mainly by the strength of the two light-induced effects, nonlinear absorption and nonlinear scattering.

Most often in what follows we refer to measurements of the transmittance dynamics from the moment B, i.e. from the time when the green preillumination is terminated after reaching a saturation value. The value of transmittance at this moment allows for estimating the light induced absorption $\Delta\alpha_{li}$, while the dynamics of beam depletion which is due to transient beam fanning (time interval C-D-E) gives information about efficiency of sensitizing and the relaxation of the secondary centers responsible for the enhanced sensitivity [5].

Qualitatively similar behavior was detected with all tested Sb-doped samples, K21, K24, and K33. The sample with the smallest thickness (K24, $d=2$ mm) was selected for further measurements because it ensured well pronounced changes in transmission in a range still far from a complete exhaustion of the transmitted beam (either because of nonlinear absorption or because of photorefractive scattering). For samples with larger thickness the processing of data obtained with intense short wavelength preillumination faced serious difficulties because the sample remained completely opaque during sufficiently long time. It should be added also that the light induced absorption and transient beam fanning were much weaker in nominally undoped sample

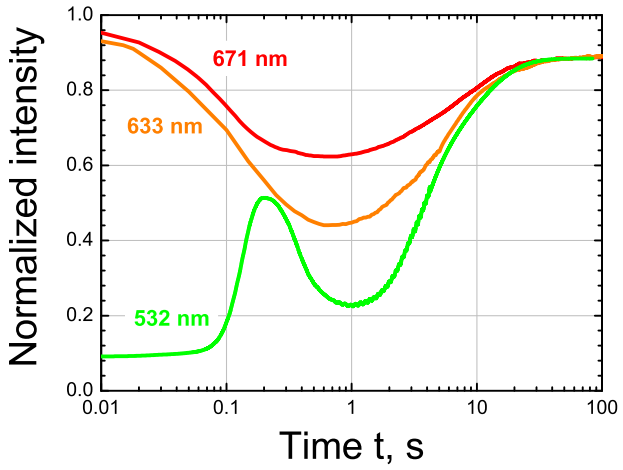

Fig. 3. Temporal variation of the red testing beam intensity in response to light preexposure with different wavelengths: 671 nm (1 W/cm^2), 633 nm (2 W/cm^2), and 532 nm (1 W/cm^2) for sample K24. The intensity of testing beam is below 70 mW/cm^2 for all three curves.

(K16), in tellurium doped (K32) and antimony-tellurium co-doped (K31) samples.

Fig. 3 shows how the intensity of the transmitted testing beam (He–Ne laser, 633 nm) changes in time if preillumination is achieved with light of the same wavelength (633 nm), shorter wavelength (532 nm), and longer wavelength (671 nm). The measurements are performed with the same sample K24. In spite of the fact that no attempts were taken to keep the same intensities or the same photon fluxes of auxiliary beams with different wavelengths, some important qualitative conclusions can be drawn from the data. First of all, the transmittance of the sample just after preillumination is the smallest for green light and tends to increase with the increasing wavelength of preexposure. Only three curves are selected in Fig. 3 to avoid data overload, but they show the tendency clearly.

The next conclusion is related to the second depletion of the testing beam, in a range of 0.5–2.0 s time delay. The depth of the second minimum in curves of Fig. 3 is a qualitative measurement of the gain factor enhancement produced by preillumination [5]. The strongest depletion occurs when the photon energy of preilluminating light is close to the crystal bandgap. It can also be seen that the development of the light induced scattering (beam fanning) which is responsible for second depletion is delayed in time for green light of preillumination because of the very strong absorption of red testing light, which persists up to 0.2–0.3 s after termination of preexposure. In spite of this partial inhibition of the beam fanning in a strongly absorbing sample, the strongest depletion because of induced scattering occurs just for the green preexposure. It seems therefore that the most efficient way to sensitize $Sn_2P_2S_6$:Sb is to use a green light for preillumination.

Some qualitative conclusions on characteristic decay times of two observed photoinduced processes can be determined from data of Fig. 3, too. For all three dependences the transmission returns back to its initial value roughly 100 s after interruption of the preexposure. Thus, the density of photoinduced secondary centers which are responsible for the enhanced sensitivity vanishes within the range from 1 to 100 s. The characteristic time that can be extracted from the tails of transmission decay is practically independent of probe beam intensity within the range from 5 to 200 mW/cm^2. For the intensities below 5 mW/cm^2 the photoconductivity decreases to the values comparable to dark conductivity, the photorefraction is inhibited and second depletion minimum becomes less pronounced. The extraction of reliable data on the decay time becomes problematic for this intensity range both, because of smaller effect and because the additional relaxation process enters into consideration.

As one can see from the data of Fig. 3 the decay times of secondary centers for different wavelengths of preexposure do not differ much, which is discussed below. The decay of the light induced absorption occurs faster than the decay of the sensitized state. This follows from the transmission curve for green preillumination: if the decay time of the centers responsible for light induced absorption would be equal or longer than the lifetime of secondary centers responsible for sensitizing, the transmission curve would feature only one unresolved minimum instead of the two clearly resolved minima in Fig. 3.

Let us turn now to the description of measurements. We started with measuring the light induced absorption $\Delta\alpha_{li}$

$$\Delta\alpha_{li} = -(1/d)\ln T_{sat}, \quad (1)$$

where T_{sat} stands for the smallest steady-state normalized transmission of the sample (T at the exposure time close but below point B in Fig. 2) and d is the illuminated layer thickness.

The intensity dependences of optical density $\Delta\alpha_{li}d$ for sample K24 (d=2 mm) are shown in Fig. 4 for three different preillumination wavelengths.

For moderate preillumination intensities they all are fairly linear. This allows for characterizing the strength of the induced absorption within this range of preillumination intensities by only one parameter $d\Delta\alpha/dI$, which itself does not depend on the preillumination intensity. Its spectral dependence is presented in Fig. 5.

The results presented in Figs. 4 and 5 are in qualitative agreement with those reported in [11,12]. The previously measured spectral dependences of the self-induced absorption also show the strongest changes near the edge of fundamental absorption, both for nominally undoped [11] and antimony doped [12] material. The nonlinear absorption decreases smoothly up to $\lambda \approx 1\,\mu$m where the sign of effect is reversed: the self-induced bleaching occurs instead of self-induced absorption. It should be underlined that the absolute values of the light induced absorption are much larger in antimony doped samples as compared to nominally undoped samples.

The spectral dependence shown in Fig. 5 resembles, in addition, the excitation spectrum of the photo-stimulated EPR signal of divalent antimony ion in SPS:Sb measured by S. Basun and D. Evans (will be published and discussed elsewhere). All these correlations

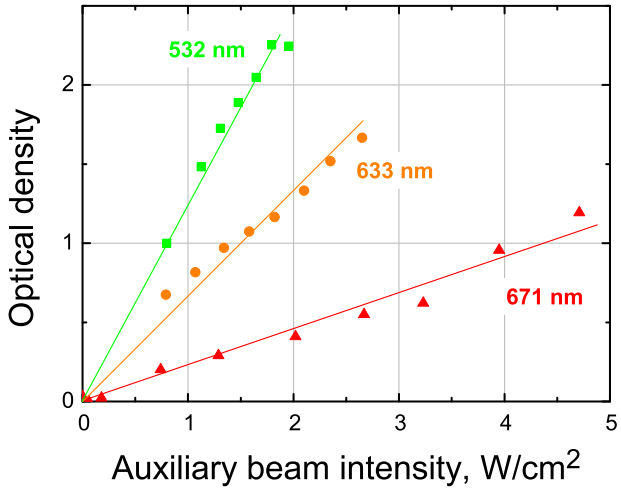

Fig. 4. Nonlinear absorption $\Delta\alpha_{li}$ times sample thickness d versus preillumination intensity I_{aux} for preillumination wavelengths 532 nm (squares), 633 nm (dots), and 671 nm (triangles); sample K24. The intensity of testing beam is below 70 mW/cm^2 for all three curves.

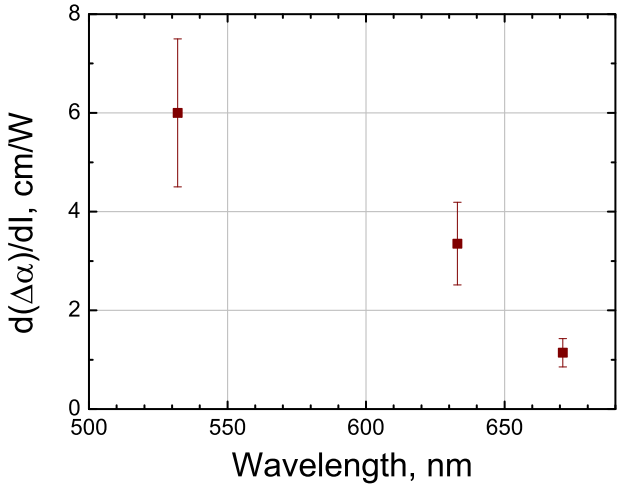

Fig. 5. The strength of light induced absorption versus the wavelengths of pre-exposure light for sample K24.

Table 1
Decay time of secondary centers for different SPS:Sb samples at different pre-exposure wavelengths.

Sample	532 nm	590 nm	633 nm	671 nm
K21	–	–	14 s	–
K24	16 s	20 s	12 s	17 s
K33	–	–	10 s	16 s

confirm the initial hypothesis that the extrinsic defects themselves (antimony) are responsible for the atypically strong light induced absorption in SPS:Sb.

The development and disappearance of the light induced absorption in SPS:Sb is quite fast, it takes a fraction of a second at ambient temperature (see Fig. 3). In a further experiment, the testing red beam was switched on with a controllable delay after termination of preexposure, during that time the SPS sample was kept in the dark. The instantaneous value of $\Delta\alpha$ was measured just when the testing red beam was switched on. (This is different from similar experiment described in Ref. [5], where the largest depletion of the testing beam was measured as a function of the dark delay time after preillumination.) A rapid decrease of absorption was detected already after the one second delay in the dark. The experiment was performed with the green light preillumination for which the nonlinear absorption is the most pronounced.

We attempted next to evaluate the relaxation time of the secondary centers for different wavelengths of preillumination. The accuracy of the decay time extraction is not very high and the spread of values for different samples is quite large. From the data summarized in Table 1 it is clearly seen that all measured values appear within the range 15 ± 5 s; they are in agreement with that reported in Ref. [5] for He–Ne laser light preillumination. We conclude therefore that whatever the quantum energy of preillumination light is (within the range shown in Fig. 5), the same secondary trap centers are activated, which enhance the photorefractive response of SPS:Sb.

4. Conclusions

The preillumination of $Sn_2P_2S_6$:Sb samples results in two distinct effects: transient photoinduced absorption (photochromism) and transient photoinduced scattering (transient beam fanning). The second effect is a consequence of light induced enhancement of photorefractive response.

Both effects are inherently related to antimony doping; they are well pronounced in crystals with 1% of Sb; a much smaller effect (or sensitizing with considerably different lifetime of secondary centers) was observed in nominally undoped $Sn_2P_2S_6$, tellurium doped $Sn_2P_2S_6$:Te1% and co-doped $Sn_2P_2S_6$:Sb:Te 0.5%, Sb 0.5% samples.

Well below the saturation level, the light induced absorption increases linearly with the intensity of preillumination; the overall effect becomes weaker with an increasing wavelength of preillumination.

The lifetime of the secondary photorefractive centers does not depend on preillumination light wavelength and falls into a range from 10 to 20 s for different samples and for different wavelengths of preillumination. The characteristic decay time of the defect centers responsible for photoinduced absorption is $\tau_a \approx 0.2$–0.3 s at ambient temperature for preillumination with green light. While the reliable data for other preillumination wavelengths are not available at present, it is clear that the photoinduced absorption always decays faster than the secondary photorefractive centers disappear. These findings allow for concluding that the photoinduced absorption and photoinduced sensitizing in $Sn_2P_2S_6$:Sb develop due to at least two different types of defect centers.

Acknowledgments

This work was supported in part by EOARD/STCU Project P585. We are grateful to A. Grabar and I. Stoyka for SPS crystals.

References

[1] S. Odoulov, A. Shumelyuk, U. Hellwig, R. Rupp, A. Grabar, I. Stoyka, J. Opt. Soc. Am. B 13 (1996) 2352.
[2] S. Odoulov, A. Shumelyuk, U. Hellwig, R. Rupp, A. Grabar, I. Stoyka, Opt. Lett. 21 (1996) 752.
[3] T. Bach, M. Jazbinsek, G. Montemezzani, P. Günter, A.A. Grabar, Y. M. Vysochanskii, J. Opt. Soc. Am. B 24 (2007) 1535.
[4] A. Grabar, M. Jazbinsek, A. Shumelyuk, Y. Vysochanskii, G. Montemezzani, P. Günter, Photorefractive effects in $Sn_2P_2S_6$ in photorefractive materials and their applications 2: materials, in: P. Günter, J.-P. Huignard (Eds.), Springer Series in Optical Sciences, vol. 114, Springer, New York, 2007, pp. 327–362.
[5] D.R. Evans, A. Shumelyuk, G. Cook, S. Odoulov, Opt. Lett. 36 (2011) 454.
[6] I.V. Kedyk, P. Mathey, G. Gadret, A.A. Grabar, K.V. Fedyo, I.M. Stoika, I.P. Prits, Y. M. Vysochanskii, Appl. Phys. B 92 (2008) 549.
[7] I.V. Kedyk, P. Mathey, G. Gadret, O. Bidault, A.A. Grabar, I.M. Stoika, Y. M. Vysochanskii, J. Opt. Soc. Am. B 25 (2008) 180.
[8] A. Shumelyuk, A. Volkov, S. Odoulov, G. Cook, D.R. Evans, Appl. Phys. B 100 (2010) 101.
[9] A. Shumelyuk, A. Volkov, S. Odoulov, A. Grabar, I. Stoyka, D.R. Evans, Opt. Express 22 (2014) 24763.
[10] A.T. Brant, L.E. Halliburton, S.A. Basun, A.A. Grabar, S.G. Odoulov, A. Shumelyuk, N.C. Giles, D.R. Evans, Phys. Rev. B 86 (2012) 134109.
[11] A. Ruediger, O. Schirmer, S. Odoulov, A. Shumelyuk, A.A. Grabar, Opt. Mat, 18 (2001) 123.
[12] P. Mathey, G. Gadret, A.A. Grabar, I. Stoika, Y.M. Vysochanskii, Opt. Commun. 300 (2013) 90.